

Therapeutic Mechanisms of Human Adipose-Derived Mesenchymal Stem Cells in a Rat Tendon Injury Model

Sang Yoon Lee,^{*†} MD, PhD, Bomi Kwon,[‡] BSc, Kyoungbun Lee,[§] MD, PhD, Young Hoon Son,^{||} PhD, and Sun G. Chung,^{‡¶#**} MD, PhD
Investigation performed at Department of Rehabilitation Medicine, Seoul National University College of Medicine, Seoul, South Korea

Background: Although survival of transplanted stem cells in vivo and differentiation of stem cells into tenocytes in vitro have been reported, there have been no in vivo studies demonstrating that mesenchymal stem cells (MSCs) could secrete their own proteins as differentiated tenogenic cells.

Purpose/Hypothesis: Using a xenogeneic MSC transplantation model, we aimed to investigate whether MSCs could differentiate into the tenogenic lineage and secrete their own proteins. The hypothesis was that human MSCs would differentiate into the human tenogenic lineage and the cells would be able to secrete human-specific proteins in a rat tendon injury model.

Study Design: Controlled laboratory study.

Methods: The Achilles tendons of 57 Sprague Dawley rats received full-thickness rectangular defects. After the modeling, the defective tendons were randomly assigned to 3 groups: (1) cell group, implantation with human adipose-derived mesenchymal stem cells (hASCs) and fibrin glue (10⁶ cells in 60 μ L); (2) fibrin group, implantation with fibrin glue and same volume of cell media; and (3) sham group, identical surgical procedure without any treatment. Gross observation and biomechanical, histopathological, immunohistochemistry, and Western blot analyses were performed at 2 and 4 weeks after modeling.

Results: hASCs implanted into the defective rat tendons were viable for 4 weeks as detected by immunofluorescence staining. Tendons treated with hASCs showed better gross morphological and biomechanical recovery than those in the fibrin and sham groups. Furthermore, the expression of both human-specific collagen type I and tenascin-C was significantly higher in the cell group than in the other 2 groups.

Conclusion: Transplantation of hASCs enhanced rat tendon healing biomechanically. hASCs implanted into the rat tendon defect model survived for at least 4 weeks and secreted human-specific collagen type I and tenascin-C. These findings suggest that transplanted MSCs may be able to differentiate into the tenogenic lineage and contribute their own proteins to tendon healing.

Clinical Relevance: In tendon injury, MSCs can enhance tendon healing by secreting their own protein and have potential as a therapeutic option in human tendinopathy.

Keywords: mesenchymal stem cells; xenogeneic stem cell transplantation; tendon injuries; Achilles tendon; collagen type I

Mesenchymal stem cell (MSC)-based therapy has been thought to induce tissue healing by 3 possible mechanisms.²³ First, MSCs may modulate immune responses through their immunomodulatory functions by direct cell-to-cell contact and release of soluble immunosuppressive factors.²² Second, MSCs could secrete a broad variety of cytokines, chemokines, and growth factors that may prevent apoptosis and promote proliferation of adjacent cells.⁸ Third, MSCs may have the capacity to differentiate into various cell lineages including bone, cartilage, tendon, fat, bone marrow stroma, and muscle.¹⁵ Among the 3

potential mechanisms, it appears essential to investigate whether the third mechanism truly plays a role, such that wounded tissues are substituted with transplanted MSCs rather than repaired by proliferated or stimulated recipient cells induced by humoral or immunologic reactions. If the third mechanism fails to work in tendon healing, there is no reason to transplant MSCs, which carry a much higher risk than the sole application of humoral factors.

In the present study, we aimed to investigate whether MSCs could differentiate into the tenogenic lineage and secrete their own proteins. To prove the cellular function of MSCs, a xenogeneic cell transplantation model was planned: human adipose-derived mesenchymal stem cells (hASCs) were transplanted into a rat tendon. We hypothesized that hASCs could differentiate into the human

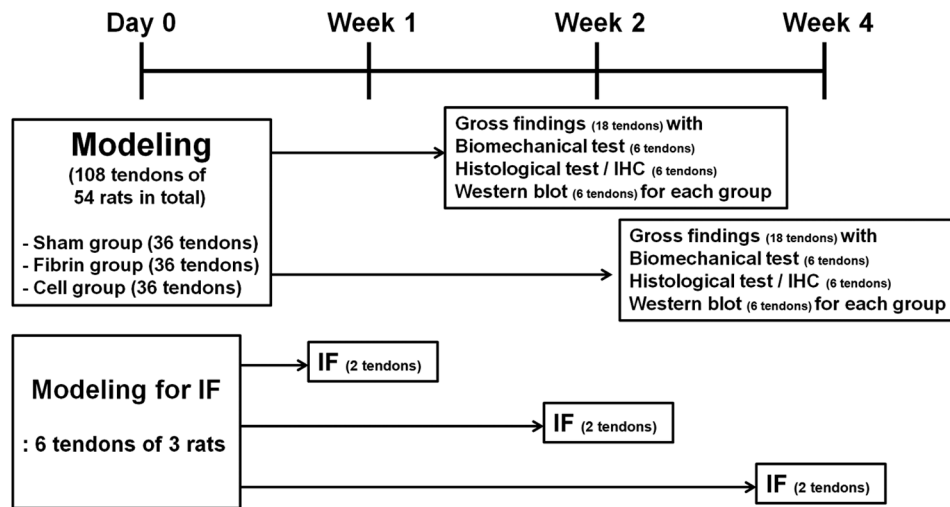


Figure 1. Flowchart of this experimental study. IHC, immunohistochemistry; IF, immunofluorescence.

tenogenic lineage and that the cells would be able to secrete human-specific proteins.

METHODS

Study Design

Fifty-seven 13-week-old male Sprague Dawley rats (body weight, 390–410 g) were used in this study. As shown in Figure 1, 54 rats were randomly divided into 3 groups: (1) cell group, implantation with hASCs and fibrin glue (10^6 cells in $60 \mu\text{L}$); (2) fibrin group, implantation with fibrin glue and same volume of cell media; and (3) sham group, identical surgical procedure without any treatment. Outcome parameters measuring the incomplete healing rate, cross-sectional area, and biomechanical and histopathological properties, as well as the results of immunohistochemistry and Western blot analysis, were assessed at 2 and 4 weeks after each modeling. Six tendons for each outcome parameter at each time point were used except for gross examination, where 18 tendons were examined at each time point. Three additional rats (6 tendons), one for each time point, were used to verify the viability of hASCs at 1, 2, and 4 weeks after cell transplantation by immunofluorescence staining. The Institutional Animal Care and Use Committee of Seoul National University Hospital approved all the procedures described below (No. 14-0242-S1A0).

Stem Cell Preparation

Preparation of stem cells was performed as described previously.¹⁰ Briefly, hASCs were isolated from lipoaspirates of human subcutaneous fat tissue obtained from healthy donors who provided informed consent. The lipoaspirates were washed with phosphate-buffered saline (PBS) and digested in PBS containing 1% bovine serum albumin and 0.025% collagenase type I (Invitrogen). The isolated stromal vascular fraction was cultured to obtain a sufficient number of cells for injection. After harvesting of cells by trypsinization, the cells were suspended and packaged into single-use vials. For lot-release testing, hASCs were assessed for cell appearance, viability, identification, purity, content, and potency. The potency was assessed as a viable cell counting. Because the total amount of viable cells that could exert their biological function was determined by a reasonable potency testing item, it was assessed as the potency of hASCs. MSC characteristics such as self-renewal, cell morphology, doubling time, karyotype, cell surface markers (CD29+, CD44+, CD73+, CD90+, and CD105+/CD 34– and CD45–), and biological function, which includes growth factor releasing and immune suppressive activity, were thoroughly tested. Fluorescence-activated cell sorting technique was also used to define MSCs. Only hASCs that met all testing requirements, including test items mentioned above, were banked after culturing. The minimum criteria for release

**Address correspondence to Sun G. Chung, MD, PhD, Department of Rehabilitation Medicine, Seoul National University Hospital, 101 Daehang-ro, Jongno-gu, Seoul, 03080, South Korea (email: suncg@snu.ac.kr).

*Department of Physical Medicine & Rehabilitation, Chung-Ang University College of Medicine, Seoul, South Korea.

†Department of Rehabilitation Medicine, Seoul National University Boramae Medical Center, Seoul, South Korea.

‡Department of Rehabilitation Medicine, Seoul National University College of Medicine, Seoul, South Korea.

§Department of Pathology, Seoul National University College of Medicine, Seoul, South Korea.

||Department of Biochemistry and Molecular Biology, Seoul National University College of Medicine, Seoul, South Korea.

*Institute of Aging, Seoul National University, Seoul, South Korea.

#Rheumatism Research Institute, Medical Research Center, Seoul National University, Seoul, South Korea.

One or more of the authors has declared the following potential conflict of interest or source of funding: This research was supported by a grant of the Korea Health Technology R&D Project through the Korea Health Industry Development Institute (KHIDI), funded by the Ministry of Health & Welfare, Republic of Korea (grant number HI12C1835).

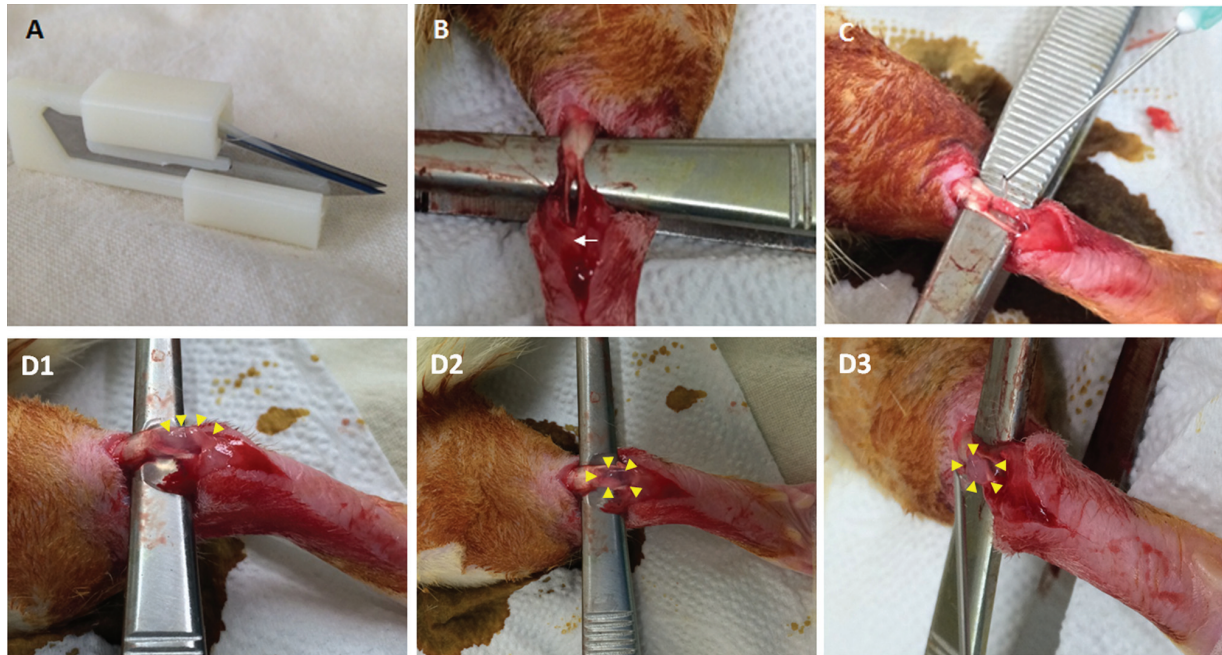


Figure 2. Intra-tendinous rectangular tendon defect and cell implantation. (A) Surgical blades assembled with plastic racks and (B) a full-thickness rectangular intratendinous defect (0.8 mm \times 5 mm) of the Achilles tendon spanning from the tendon-bone insertion at the calcaneus (arrow) to the midtendon. (C) Inoculation of human adipose-derived mesenchymal stem cells with fibrin glue into the intratendinous defect, and (D1, D2, and D3) the coagulated injectates (yellow arrowheads) before the skin closure.

were 80% cell viability and less than 1% CD45-positive cells (a measure of purity). In addition, hASCs were screened for contamination with adventitious agents, mycoplasma, bacteria, fungi, and viruses 3 days before packaging to comply with the recommendation of the Guidance on Specifications and Test Methods for Cell Therapy Products from the Korean Food and Drug Administration.

Fluorescent Cell Labeling and Immunofluorescence Staining

To distinguish between implanted hASCs and host-derived proliferated rat cells, hASCs were labeled by use of chloromethyl-1,1-dioctadecyl-3,3,3',3'-tetramethylindocarbocyanine perchlorate (CM-Dil) (C7001, CellTracker; Invitrogen Life Technologies) according to a modification of the manufacturer's protocol. Briefly, a 1 mg/mL CM-Dil stock solution was used to prepare an 8- μ M solution in 500 μ L of Hanks balanced salt solution (HBSS; Sigma-Aldrich), which was then vortexed and combined with 2×10^6 hASCs in 500 μ L HBSS, to give 10^6 cells/mL in a 4- μ M CM-Dil labeling solution. After harvesting of each tissue, the specimens were fixed and sequentially immersed in a 10%, 20%, and 30% sucrose solution for 24 hours each. After the sucrose was removed, the tissues were embedded in optimal cutting temperature and stored at -70°C in a liquid nitrogen tank. Blocks were cut into 5- μ m-thick cryostat sections and mounted on superfrost slides. We used 4',6-diamidino-2-phenylindole (DAPI) (Vector Laboratories) as a nuclear counterstain. Specific fluorescence was analyzed by use of laser scanning microscopy (BX-UCB; Olympus Co).

Surgical Procedure and Treatment

Anesthesia was induced and maintained with 5% and 2% isoflurane dissolved in 40%:60% and 25%:75% oxygen-nitrogen applied via a chamber and nose cone, respectively. Surgical procedures were performed under sterile conditions in the prone position. An approximately 15-mm horizontal skin incision was made on the medial side over the Achilles tendon with a No. 10 surgical blade. After the tendon was completely exposed, 2 No. 11 surgical blades assembled on a plastic rack printed on a 3-dimensional (3D) printer (Figure 2A) were used to make a standardized parallel incision in the tendon 0.8 mm apart and 5 mm long, spanning from the tendon-bone insertion at the calcaneus to the midtendon. To induce rectangular defects, micro-scissors were used to remove the scored sections, such that a full-thickness defect was created in the midsubstance⁷ (Figure 2B). Then, a 60- μ L volume of mixtures with 10^6 hASCs and fibrin glue was inoculated into the intratendinous defect in the cell group. A dual-syringe injection system (Greenplast kit, Green Cross) with 26-gauge needles was loaded with 30 μ L of thrombin mixed with 10^6 hASCs in the first syringe and 30 μ L of fibrinogen in the other syringe (Figure 2, C and D). In the fibrin group, the defect was filled with the same volume (60 μ L) of fibrin glue and cell media. An identical surgical procedure without any treatment was conducted in the sham group. After the modeling of one hindlimb in each rat was finished, the same procedure and the same inoculated materials were applied to the other hindlimb. All rats received subcutaneous injections with 1 mg/kg meloxicam

and 20 mg/kg cefazolin for 3 days (1 hour before and 1 day and 2 days after the operation).

Gross Measurements

Rats were euthanized by means of carbon dioxide inhalation, and tendons were harvested at 2 and 4 weeks after modeling. Incomplete healing was defined as 1 mm or more of visible gapping between the tendon end and the calcaneal bone with partial or complete loss of continuity.²⁷ Assuming the cross section of a tendon was an ellipse, tendon cross-sectional area at the midportion of the surgical defect was calculated by 2 perpendicular thickness axes (major axis = a and minor axis = b) as follows: cross-sectional area = $\pi \times a \times b/4$.^{2,13} Each thickness was measured by a digital vernier caliper.

Biomechanical Test

Tendons for the biomechanical test (6 tendons in each group at each time point; 36 tendons in total) were harvested still attached to the foot, and the triceps surae muscle was transected through the muscle belly, well proximal to the tendon repair. All the harvested specimens were stored at -80°C to prevent tissue damage. Before the test, tissues were thawed at room temperature for more than 4 hours. Each thawed Achilles tendon was moistened with gauzes soaked in PBS solution to prevent drying out. The distal end around the metatarsal bone was securely press-fixed with a metallic clamp while the proximal end (triceps surae muscle) was frozen with liquid nitrogen and fixed in a customized frame produced by a 3D-printer (Figure 3). To ensure that the liquid nitrogen did not affect the healed tendon itself, the surface temperature of the tendons was measured before and after liquid nitrogen application. The temperature difference was less than 2°C in all specimens. The tendons were then mounted onto a biomechanical testing machine (JSV-H100; JISC) with a 100-N load cell. The construct was initially set to a basic axial stress of 0.1-N preload for straightening and adjustment. After that, the length between the calcaneal bone and the myotendinous junction was measured as an initial length. Each tendon was then axially pulled at a constant speed of 10 mm/min until maximal load to failure. Ultimate tensile strength (N), stiffness (N/mm), and Young's modulus (MPa or N/mm^2) were measured from each tendon's stress-strain curve.⁹

Tissue Preparation and Histological Analysis

Achilles tendons for histological analysis and immunohistochemistry were harvested between the calcaneus and the musculotendinous junction. After fixing in 10% formalin for a day, the specimens were embedded in paraffin, cut into 3- μm coronal sections, and stained with either hematoxylin and eosin (H&E) or Alcian blue. Histopathological analysis of the Achilles tendon was performed on the stained tissue by use of the semiquantitative histopathological scale (modified Bonar score).⁴

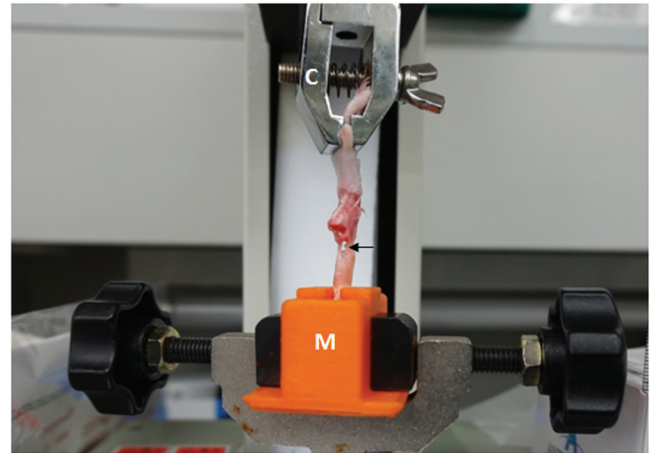


Figure 3. Two clamps for biomechanical testing and a ruptured tendon during the test. The distal end (metatarsal bone) was securely press-fixed with metallic clamp (C) while the proximal end (triceps surae muscles) was frozen in a customized mold (M). A black arrow shows the torn area of the osteotendinous junction during biomechanical test.

Immunohistochemistry

The distribution of collagen type I (COL1), collagen type III (COL3), and tenascin-C (TnC) was assessed by means of immunohistochemical (IHC) staining. To evaluate whether COL1 is synthesized by the differentiated hASCs (donor) or already present in rat cells (recipient), 2 antibodies were used: a human-specific anti-COL1 monoclonal antibody (ab138492; Abcam) or a general anti-COL1 polyclonal antibody (ab84956; Abcam) that detects both human and rat COL1. A general anti-COL3 polyclonal antibody (ab23746; Abcam) and a human-specific anti-TnC monoclonal antibody (ab58954; Abcam) were also used. Slides were stained using the Discovery XT automated immunohistochemistry stainer (Ventana Medical Systems). The glass slides were then examined using an Olympus BX51 microscope (Olympus Co). The photographs of the specimens under $\times 400$ magnification were taken in 10 different fields using the Leica Application Suite EZ (Leica). Human skin was used as a positive control in human-specific protein analyses. After the IHC staining, sections stained with each antibody were quantitatively analyzed in a random order with ImageJ (National Institutes of Health, <http://rsb.info.nih.gov/ij/>) by color deconvolution with 10 high-power fields ($\times 400$) as reported previously.²⁵ To determine the correct optical density vectors for the red-green-blue channel of hematoxylin and 3,3'-diaminobenzidine, the protocol previously described by Ruifrok and Johnston¹⁶ was followed.

Western Blot Analysis

From each tendon, 30 to 40 mg of total protein was extracted by homogenization with the Pro-Prep protein extraction solution (iNtRON Biotechnology). Homogenates

TABLE 1
Incomplete Healing Rates in Each Group

Time Point	Sham Group, % (n/N)	Fibrin Group, % (n/N)	P Value ^a	Cell Group, % (n/N)	P Value ^a	P Value ^b
2 wk	16.7 (3/18)	22.2 (4/18)	.674	5.6 (1/18)	.289	.148
4 wk	33.3 (6/18)	22.2 (4/18)	.457	16.7 (3/18)	.248	.674
Total	25.0 (9/36)	22.2 (8/36)	.781	11.1 (4/36)	.126	.206

Compared with ^asham and ^bfibrin group at the same period (by chi-square test).

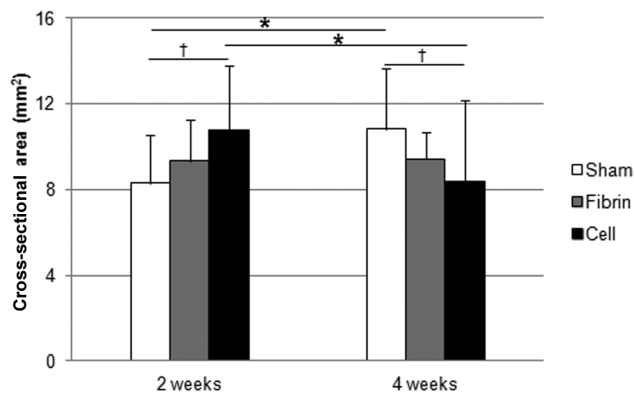


Figure 4. Cross-sectional areas of rat tendons in each group. $P < .05$ by post hoc test using Fisher least significant difference after analysis of variance compared with *the same group at 2 weeks and with †the sham group at the same period.

were centrifuged at 13,000g at 4°C for 30 minutes. The protein concentration in the homogenates was measured by means of the BCA protein assay reagent (Pierce). After gel electrophoresis and transfer of the proteins, they were detected with the following primary antibodies: human-specific anti-COL1 (ab138492; Abcam), general anti-COL1 (ab6308; Abcam), general anti-COL3 (MAB3580; Anova), anti-matrix metalloproteinase 2 (MMP-2) (ab86607; Abcam), anti-matrix metalloproteinase 9 (MMP-9) (ab76003; Abcam), and monoclonal anti- α tubulin produced in mouse (T9026; Sigma-Aldrich). Signal bands were detected using a chemiluminescence kit (Pierce) and quantified with ImageJ. For each protein, the ratio of band intensity to α -tubulin intensity was calculated.

Statistical Analysis

Differences in incomplete healing rates between the 2 groups were analyzed by chi-square tests. The cross-sectional area of tendon among the 3 groups was compared by use of analysis of variance and Fisher least significant difference post hoc test. Because the sample size of each outcome variable was not large enough, the Kruskal-Wallis test was used to compare the results of biomechanical, histological, and optical densities from IHC and Western blot among the 3 groups. The Mann-Whitney *U* test was also used for post hoc comparisons between the 2 groups. All

statistical analyses were performed with PASW Statistics 18.0 for Windows (SPSS). P values $< .05$ were considered to be statistically significant.

RESULTS

Gross Findings

Determined at 2 and 4 weeks, the incomplete healing rate of the cell group (11.1%) tended to be lower than the rates of the sham (25.0%) and fibrin (22.2%) groups, although the differences were not statistically significant ($P = .126$ and $P = .206$, respectively) (Table 1). In the cell group, cross-sectional area at 4 weeks was lower than that at 2 weeks (8.4 ± 3.8 vs 10.7 ± 3.0 mm²; $P = .008$). In the sham group, cross-sectional area at 4 weeks was higher than that at 2 weeks (10.8 ± 2.8 vs 8.3 ± 2.3 mm²; $P = .005$), whereas cross-sectional areas of the fibrin group were comparable between the 2 time points (9.3 ± 1.9 vs 9.4 ± 1.2 mm²; $P = .949$) (Figure 4).

Biomechanical Test

During the biomechanical test, 6 specimens (2 in the sham group, 3 in the fibrin group, and 1 in the cell group) slipped out of the plastic frame. In all such slippages, the proximal end of the muscle slipped out of the plastic frame. Therefore, 30 specimens were eventually analyzed for the biomechanical test.

In the cell group, stiffness at 4 weeks was higher than that at 2 weeks (19.9 ± 6.0 vs 10.1 ± 3.9 N/mm, $P = .010$). Although differences were found in both the ultimate tensile strength and Young’s modulus in the cell group, these were not significant ($P = .055$ and $P = .078$, respectively). In biomechanical variables, stiffness was the only parameter significantly different among the 3 groups at 2 weeks ($P = .012$). Ultimate tensile strength and stiffness of the cell group were significantly higher than those of the sham group at 2 weeks (49.4 ± 17.4 N vs 31.2 ± 7.5 N, $P = .037$, and 10.1 ± 3.9 N/mm vs 4.7 ± 1.4 N/mm, $P = .010$, respectively). The stiffness values of the cell group at 2 and 4 weeks were also significantly higher than those of the fibrin group ($P = .037$ in both) (Figure 5).

Histological Analysis (Modified Bonar Score)

The longitudinal defect and recovered tissue were histologically revealed by both H&E and Alcian blue staining

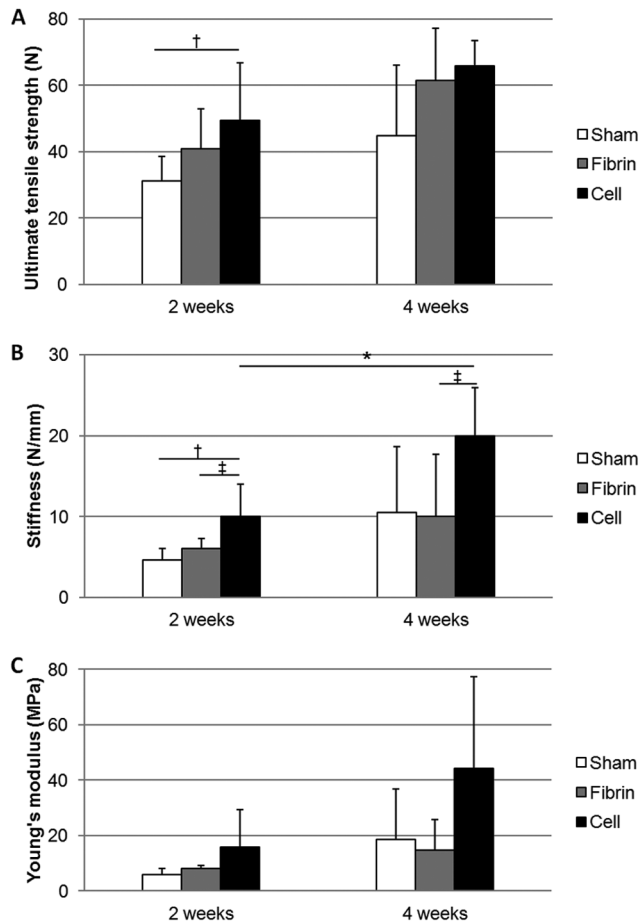


Figure 5. Three biomechanical properties of each group. (A) Ultimate tensile strength, (B) stiffness, and (C) Young's modulus. $P < .05$ by Mann-Whitney U test compared with *the same group at 2 weeks and the †sham and ‡fibrin groups at the same period.

(Figure 6, A and B). For each group, the total modified Bonar scores at 2 weeks were not different from those at 4 weeks. Among the 3 groups, the scores were significantly different at 2 weeks ($P = .045$) but not at 4 weeks ($P = .355$). At 2 weeks, the sham group showed significantly lower scores than the fibrin group ($P = .022$) (Figure 6C).

Immunohistochemistry and Immunofluorescence Staining

In each group, the optical densities of general COL1 staining at 2 weeks were not different from those at 4 weeks. Among the 3 groups, the optical densities of general COL1 were also not different at either 2 or 4 weeks ($P = .103$ and $P = .472$, respectively). However, the cell group tended to have higher optical densities of general COL1 than the sham and fibrin groups at both 2 weeks ($P = .077$ and $P = .355$, respectively) and 4 weeks ($P = .355$ and $P = .289$, respectively), although the findings were not statistically significant (Figure 7A). In the general COL3 staining,

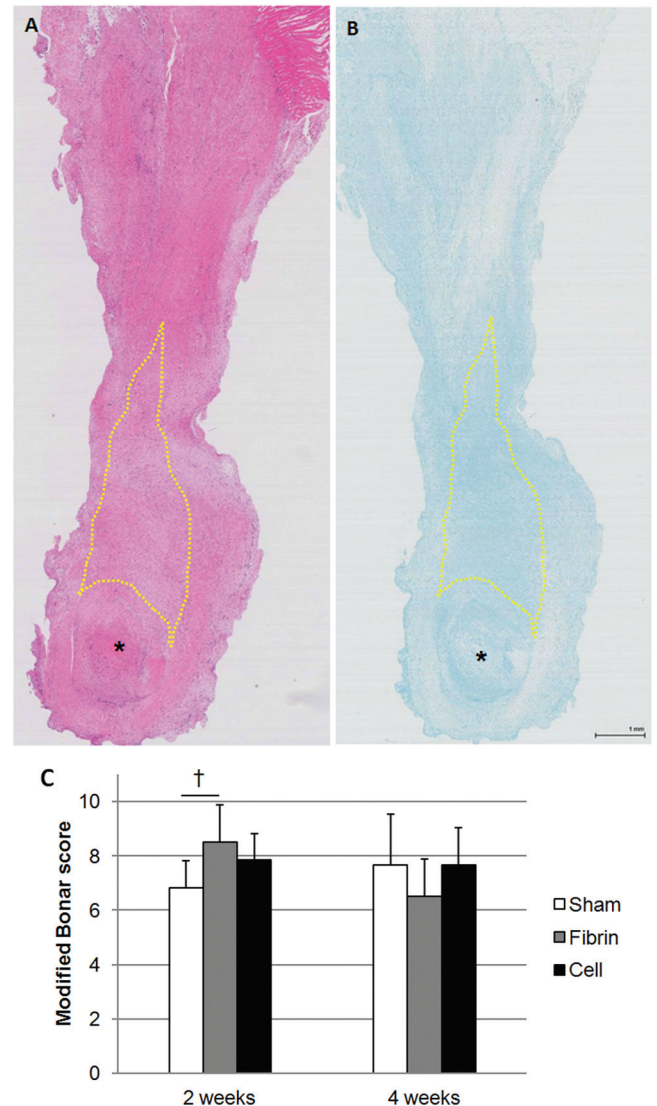


Figure 6. Histological analysis. Representative sections in sham group (midcoronal section, magnification $\times 40$) after 2 weeks from modeling with (A) hematoxylin and eosin (H&E) staining and (B) Alcian blue staining. Dotted polygons represent the hypothetical intratendinous defect that was recovering histologically, and asterisks represent the core of calcaneal bone. (C) Histopathological outcomes by modified Bonar score. $P < .05$ by Mann-Whitney U test compared with †the sham group at the same period.

only the cell group showed different optical densities between 2 and 4 weeks ($P = .037$). Among the 3 groups, optical densities of general COL3 were not significantly different at either 2 or 4 weeks ($P = .372$ and $P = .076$, respectively). However, the cell group tended to have a lower optical density of COL3 than the sham and fibrin groups at 4 weeks ($P = .037$ and $P = .078$, respectively) (Figure 7B).

In the human-specific COL1 staining, the optical densities were significantly different at both 2 and 4 weeks ($P = .004$ and $P = .020$, respectively) among the 3 groups. The

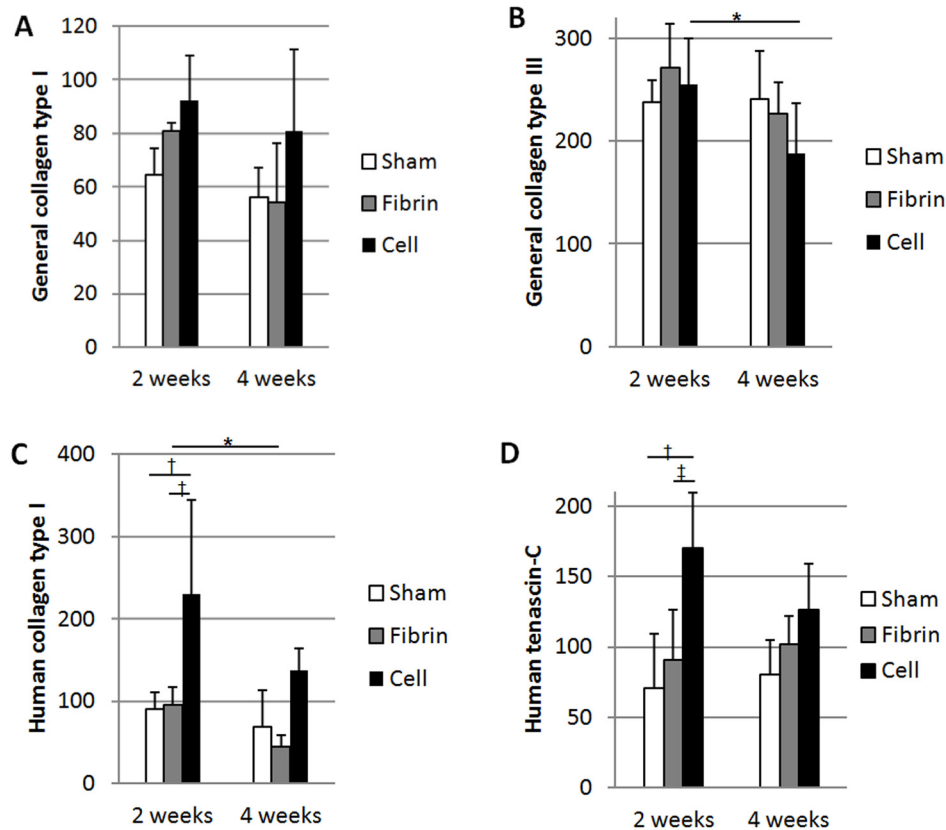


Figure 7. Quantification of 4 proteins by immunohistochemistry. (A) General collagen type I, (B) general collagen type III, (C) human-specific collagen type I, and (D) human-specific tenascin-C antibodies. $P < .05$ by Mann-Whitney U test compared with *the same group at 2 weeks and with the †sham and ‡fibrin groups at the same period.

cell group had significantly higher optical densities at both 2 and 4 weeks did the sham ($P = .004$ and $P = .033$, respectively) and fibrin groups ($P = .006$ and $P = .011$, respectively) (Figure 7C, 8A, and 8B). In human-specific TnC staining, all groups had similar optical densities between 2 and 4 weeks. Among the 3 groups, the optical densities of human-specific TnC were significantly different only at 2 weeks ($P = .012$). The cell group showed a higher optical density than did the sham and fibrin groups ($P = .009$ and $P = .028$, respectively) at 2 weeks. At 4 weeks, the optical densities of human-specific TnC in the cell group also tended to have higher values than those in the sham and fibrin groups ($P = .050$ and $P = .327$, respectively), although these differences were not significant (Figure 7D, 8C, and 8D).

Immunofluorescence staining revealed that the CM-Dil-labeled hASCs remained viable in host rat tendons at 1, 2, and 4 weeks after cell implantations (Figure 9).

Western Blot Analysis

Western blot analysis revealed no differences in the expression of general COL1 between 2 and 4 weeks in all groups. Among the 3 groups, differences in protein expression of general COL1 were not significant at either 2 or 4 weeks (Figure 10A). Human-specific COL1 expression in

the sham group was different between 2 and 4 weeks ($P = .034$). Among the 3 groups, human-specific COL1 expression was different only at 4 weeks ($P = .023$), being higher in the cell and fibrin groups than in the sham group ($P = .021$ in both) (Figure 10B).

MMP-2 expression in both the fibrin and cell groups at 4 weeks was lower than at 2 weeks ($P = .004$ and $P = .014$, respectively). Among the 3 groups, differences were noted at both 2 and 4 weeks ($P = .008$ and $P = .047$, respectively). Protein expression of MMP-2 in the cell group was higher than in the sham group at both 2 and 4 weeks ($P = .009$ and $P = .033$, respectively) (Figure 10C). Only the cell group showed a significant difference in MMP-9 expression between 2 and 4 weeks ($P = .034$). At 4 weeks, MMP-9 expression in the cell group was higher than in the fibrin group ($P = .011$) (Figure 10D).

DISCUSSION

The most important findings of this study were that tendons treated with human MSCs (hMSCs) showed better gross morphological and biomechanical recovery than those in the fibrin and sham groups. Furthermore, hMSCs implanted to the rat tendon defect model survived for at least 4 weeks and secreted human-specific collagen type I

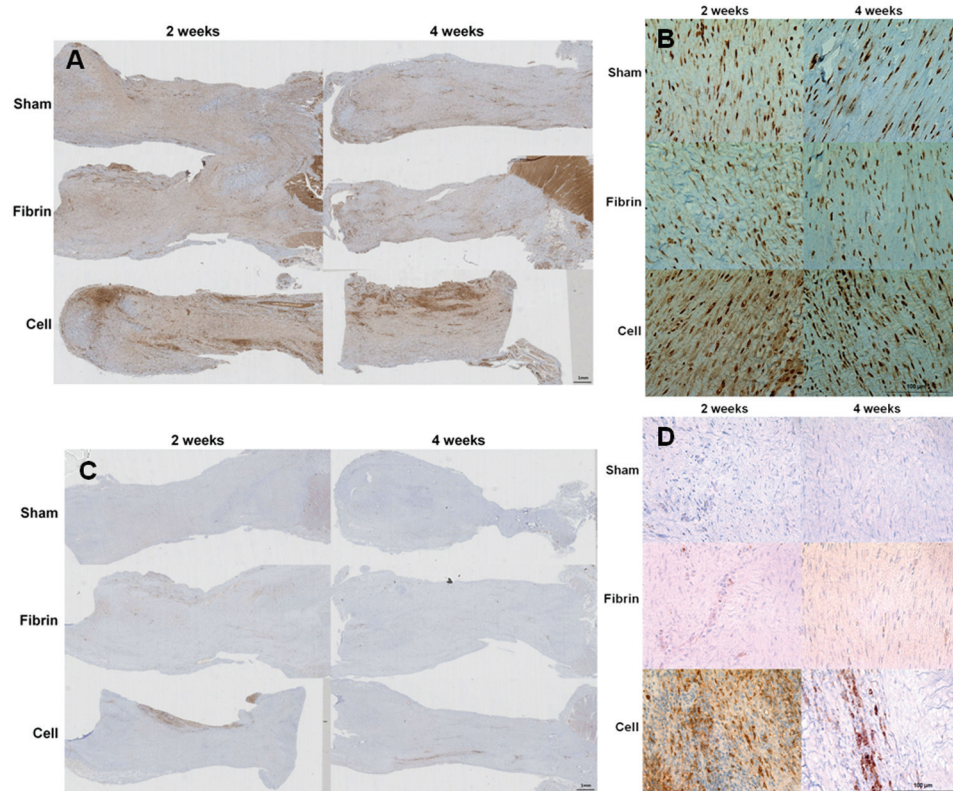


Figure 8. Immunostaining for human-specific collagen type I and tenascin-C. Immunohistochemically stained representative images with (A and B) human-specific collagen type I and (C and D) tenascin-C antibodies of 3 groups at both 2 and 4 weeks after modeling (magnification: left column $\times 40$ and right column $\times 400$).

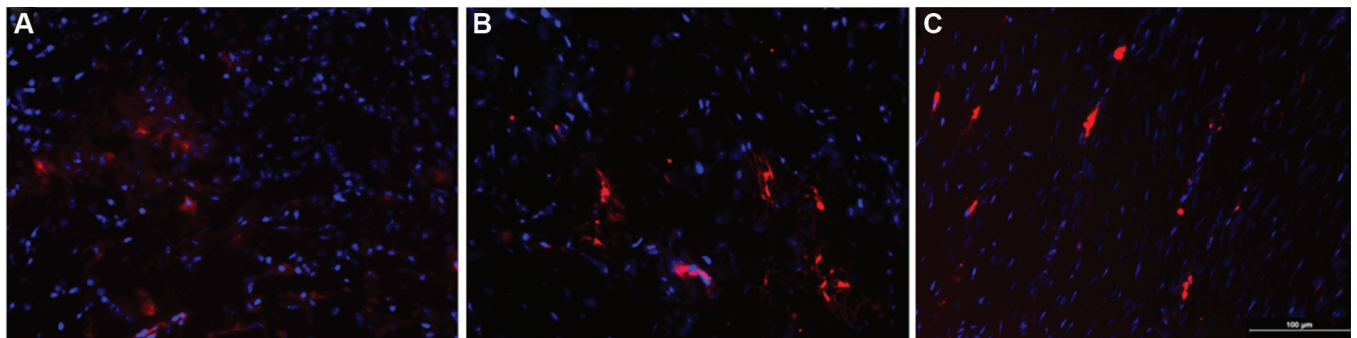


Figure 9. Fluorescently labeled human adipose-derived mesenchymal stem cells. Immunofluorescence images (magnification $\times 200$) of chloromethyl-1,1-dioctadecyl-3,3,3',3'-tetramethylindocarbocyanine perchlorate (CM-Dil) (red) tagged human adipose-derived mesenchymal stem cells at (A) 1 week, (B) 2 weeks, and (C) 4 weeks from cell implantation. All images were merged with nuclear counterstained images with 4',6-diamidino-2-phenylindole (DAPI) (blue).

and tenascin-C. Evidence from this *in vivo* xenogeneic cell transplantation model proves that hMSCs can survive for at least 4 weeks after implantation and secrete their own proteins.

hMSCs implanted onto rat Achilles tendon defects resulted in an accelerated repair as compared with application of fibrin glue only or sham treatment investigated in this study.

Morphologically, changes in the thickness of injured tendons demonstrated interesting patterns depending on treatment group. The cross-sectional areas of injured tendons in the cell group were significantly decreased from 2 to 4 weeks, whereas those in the sham group were increased and those in the fibrin group remained unchanged (Figure 4). Although all of the injured tendons in the 3 groups were thicker than

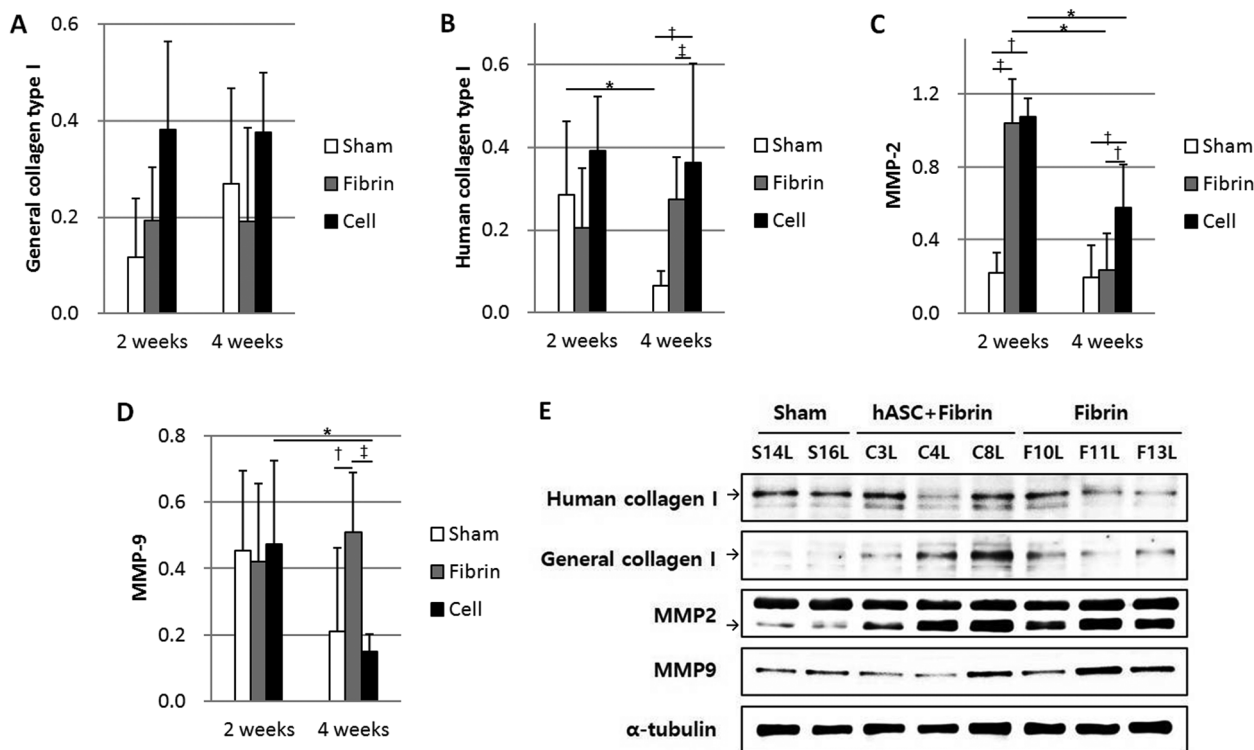


Figure 10. Quantification of 4 proteins by Western blot. (A) General collagen type I, (B) human-specific collagen type I, (C) matrix metalloproteinase 2 (MMP-2), (D) matrix metalloproteinase 9 (MMP-9) (normalized by the value of α -tubulin), and (E) representative Western blot bands. $P < .05$ by Mann-Whitney U test compared with *the same group at 2 weeks and with the †sham and ‡fibrin groups at the same period.

normal cross-sectional areas of Sprague Dawley rats ($6.0 \pm 1.4 \text{ mm}^2$),⁵ the decrease of cross-sectional areas from 2 to 4 weeks in only the cell group can be considered as a higher degree of tendon remodeling^{3,19} or an improvement of tendon edema.⁶ Kavaguchi De Grandis et al⁶ demonstrated that the cross-sectional area of digital flexor tendons became largest at day 21 and decreased by day 42 in a goat tendon defect model, indicating that tendon swelling after injury was reduced to normal as the healing process progressed. This could be interpreted as an acceleration of tendon healing in the cell group by postulating that the inflammatory phase of the cell group might have ended earlier than in the other groups.

The improved morphological repair in the cell group was corroborated by the biomechanical results showing a substantially stronger resistance to tensile load in the cell group than in the other groups at 2 and 4 weeks. Three parameters, ultimate tensile strength, stiffness, and Young's modulus, were measured to compare the degree of mechanical healing among the 3 groups. Significant differences were found in stiffness at both 2 and 4 weeks, while ultimate tensile strength did not differ meaningfully. However, the ultimate tensile strength is not considered to reflect the degree of regeneration, because our tendon defect model is basically a partial and intramural defect, depending mostly on the intact tendon tissues remaining in each side of the rectangular defect rather than on the feeble and immature tissues,

newly regenerated in the defect to generate ultimate tensile strength immediately before rupture. Yet, the feeble, immature, and regenerated tendon tissues could be more likely to contribute to stiffness, along with their neighboring healthy tendon fibers, because the property would include the mechanical behavior of the tendon while it was strained from very low to high force. Therefore, the increase of stiffness in the cell group should be interpreted as a meaningful mechanical advantage over the other 2 groups.

The more favorable healing process in the cell group was also supported by the molecular results. General COL3 expression decreased from 2 to 4 weeks in the cell group, whereas this pattern was not typically observed in the other groups. It is important to consider that the types of collagen fibers in a repaired tendon are known to be different from those of a normal tendon because the proportion of COL3 is increased to 20% to 30%.²⁶ Thus, the changing patterns in COL3 expression levels in the cell group can be interpreted as evidence of a more favorable recovery. In addition, the cell group's level of MMP-2, which participates in both collagen degradation and remodeling, was significantly higher than in the other groups, whereas a significant temporal reduction of MMP-9, which participates in collagen degradation only,^{14,18} was observed only in the cell group. From these phenomena, it could be established that the resilient power of the injured tendon in the cell group was also stronger than that in the other groups.

In our study, TnC was used as a marker to identify cells differentiating into the tenogenic lineage. Expression of TnC increased rapidly during the early period of recovery after tendon injuries, and the increase in the expression of this protein may be a necessary process in the remodeling of the tendon.¹² Because the anti-TnC antibody used in this study was specifically human-reactive, the stronger optical densities measured by IHC in the cell group should reflect the cellular function of the tenogenically differentiated human cells. Therefore, the far stronger optical densities of human-specific COL1 and TnC in the cell group indicate that implanted hASCs could secrete human-specific proteins in rat tendons. These results support the notion that the transplanted hASCs survived in tendon defects, differentiated into the tenogenic lineage, and functionally contributed their own proteins to participate in the tendon repair process. Although MSC concentration could decrease after implantation, it does not mean that all of the cells have died. Toupet et al²¹ reported that 15% of hASCs implanted in mouse joints survived during the first month, and 1.5% were still detected at 6 months. New techniques for scaffolds¹ and MSC culture conditions²⁰ to promote proliferation and survival of MSCs are currently under development. Thus, we anticipate that secreted proteins from longer surviving MSCs might function and contribute more to tissue healing in the near future.

The differentiation of MSCs into tenocytes has been studied through in vitro experiments. After BMP-12 gene transfection by electroporation, the morphology of rhesus bone marrow-derived MSCs has been changed to resemble the tenocyte shape.²⁴ Schneider et al¹⁷ reported that canine adipose tissue-derived MSCs differentiated into tenocytes after a high-density co-culture with primary tenocytes. However, in the in vivo conditions as used in our study, differentiated cells from the implanted MSCs might have been difficult to detect because the recipient tissues are also abundant in already differentiated cells. Therefore, we designed a xenogeneic MSC transplantation model to distinguish between the differentiated cells from human-donor MSCs and recipient cells of rat tendon by using species-specific antibodies of cell markers.

Although human-specific monoclonal antibodies were used to detect human proteins, the tendon tissues in the sham and fibrin groups, which had no human cells, were also weakly stained by the antibodies owing to interspecies cross-reactivity. It could be possible that the increased staining of human protein in the cell group was simply due to the implanted cells inducing collagen expression in the host rat cells through paracrine effects rather than due to the cells themselves producing the human-specific collagen. However, the optical densities of human-specific COL1 and TnC in the cell group were immensely stronger than those in the other groups, and the intergroup differences in human-specific COL1 were also confirmed by Western blot. Therefore, we suggest that implanted human stem cells can secrete human-specific proteins in the rat tendon.

There are several limitations in this study. First, a long-term effect of MSCs exceeding 4 weeks was not examined since merely 2 time points (2 and 4 weeks after modeling)

were investigated. Whether the cells can survive and the secreted human-specific proteins will not cause an immunological rejection beyond 4 weeks should be investigated in the future to confirm the efficacy and safety of MSCs. Therefore, studies with a longer follow-up period are needed to draw a general conclusion. Second, genetic expression levels of collagens and TnC were not studied. Reverse transcription-polymerase chain reaction (RT-PCR), which can measure specific messenger RNA (mRNA) expression, will be helpful to verify the differentiation of MSCs into the tenogenic lineage.¹¹ Although protein synthesis, which was mainly investigated in the current study, is the last step of the central dogma of molecular biology—DNA makes RNA makes protein, further studies investigating other genetic or cellular factors are needed to reinforce the results of the current study. Third, no significant histopathological improvements were observed in any of the groups, based on the modified Bonar scores. Because the score was originally designed for assessment of patellar tendinopathy,⁴ a quintessentially chronic overuse condition, this might not have been an appropriate measure to delineate histopathological recovery from acute damage, as investigated in the current study.

In conclusion, transplantation of hASCs enhanced rat tendon healing biomechanically. hASCs implanted into the rat tendon defect model survived for at least 4 weeks and secreted human-specific COL1 and TnC. These findings suggest that transplanted MSCs may be able to differentiate into the tenogenic lineage and contribute their own proteins to tendon healing.

REFERENCES

- Blocki A, Beyer S, Dewavrin JY, et al. Microcapsules engineered to support mesenchymal stem cell (MSC) survival and proliferation enable long-term retention of MSCs in infarcted myocardium. *Biomaterials*. 2015;53:12-24.
- Brown TD, Fu FH, Hanley EN Jr. Comparative assessment of the early mechanical integrity of repaired tendon Achilles ruptures in the rabbit. *J Trauma*. 1981;21(11):951-957.
- Daher RJ, Chahine NO, Razzano P, Patwa SA, Sgaglione NJ, Grande DA. Tendon repair augmented with a novel circulating stem cell population. *Int J Clin Exp Med*. 2011;4(3):214-219.
- Fearon A, Dahlstrom JE, Twin J, Cook J, Scott A. The Bonar score revisited: region of evaluation significantly influences the standardized assessment of tendon degeneration. *J Sci Med Sport*. 2014;17(4):346-350.
- Hammerman M, Aspenberg P, Eliasson P. Microtrauma stimulates rat Achilles tendon healing via an early gene expression pattern similar to mechanical loading. *J Appl Physiol (1985)*. 2014;116(1):54-60.
- Kavaguchi De Grandis A, Boulocher C, Viguier E, Roger T, Sawaya S. Ultrasonograph and clinical quantitative characterization of tendinopathy by modified splitting in a goat model. *Scientific World Journal*. 2012;2012:472023.
- Kim MY, Farnebo S, Woon CY, Schmitt T, Pham H, Chang J. Augmentation of tendon healing with an injectable tendon hydrogel in a rat Achilles tendon model. *Plast Reconstr Surg*. 2014;133(5):645e-653e.
- Kinnaird T, Stabile E, Burnett MS, et al. Marrow-derived stromal cells express genes encoding a broad spectrum of arteriogenic cytokines and promote in vitro and in vivo arteriogenesis through paracrine mechanisms. *Circ Res*. 2004;94(5):678-685.
- Kraus TM, Imhoff FB, Wexel G, et al. Stem cells and basic fibroblast growth factor failed to improve tendon healing: an in vivo study using lentiviral gene transfer in a rat model. *J Bone Joint Surg Am*. 2014;96(9):761-769.

10. Lee SY, Kim W, Lim C, Chung SG. Treatment of lateral epicondylitis by using allogeneic adipose-derived mesenchymal stem cells: a pilot study. *Stem Cells*. 2015;33(10):2995-3005.
11. Morita Y, Watanabe S, Ju Y, Xu B. Determination of optimal cyclic uniaxial stretches for stem cell-to-tenocyte differentiation under a wide range of mechanical stretch conditions by evaluating gene expression and protein synthesis levels. *Acta Bioeng Biomech*. 2013;15(3):71-79.
12. Nemoto M, Kizaki K, Yamamoto Y, Oonuma T, Hashizume K. Tenascin-C expression in equine tendon-derived cells during proliferation and migration. *J Equine Sci*. 2013;24(2):17-24.
13. Noguchi M, Kitaura T, Ikoma K, Kusaka Y. A method of in-vitro measurement of the cross-sectional area of soft tissues, using ultrasonography. *J Orthop Sci*. 2002;7(2):247-251.
14. Oshiro W, Lou J, Xing X, Tu Y, Manske PR. Flexor tendon healing in the rat: a histologic and gene expression study. *J Hand Surg Am*. 2003;28(5):814-823.
15. Pittenger MF, Mackay AM, Beck SC, et al. Multilineage potential of adult human mesenchymal stem cells. *Science*. 1999;284(5411):143-147.
16. Ruifrok AC, Johnston DA. Quantification of histochemical staining by color deconvolution. *Anal Quant Cytol Histol*. 2001;23(4):291-299.
17. Schneider PR, Buhrmann C, Mobasheri A, Matis U, Shakibaei M. Three-dimensional high-density co-culture with primary tenocytes induces tenogenic differentiation in mesenchymal stem cells. *J Orthop Res*. 2011;29(9):1351-1360.
18. Sharma P, Maffulli N. Current concepts review tendon injury and tendinopathy: healing and repair. *J Bone Joint Surg Am*. 2005;87(1):187-202.
19. Sharma P, Maffulli N. Biology of tendon injury: healing, modeling and remodeling. *J Musculoskelet Neuronal Interact*. 2006;6(2):181-190.
20. Somaiah C, Kumar A, Mawrie D, et al. Collagen promotes higher adhesion, survival and proliferation of mesenchymal stem cells. *PLoS One*. 2015;10(12):e0145068.
21. Toupet K, Maumus M, Peyrafitte JA, et al. Long-term detection of human adipose-derived mesenchymal stem cells after intraarticular injection in SCID mice. *Arthritis Rheum*. 2013;65(7):1786-1794.
22. Uccelli A, Moretta L, Pistoia V. Mesenchymal stem cells in health and disease. *Nat Rev Immunol*. 2008;8(9):726-736.
23. Wang J, Liao L, Tan J. Mesenchymal-stem-cell-based experimental and clinical trials: current status and open questions. *Expert Opin Biol Ther*. 2011;11(7):893-909.
24. Wang QW, Chen ZL, Piao YJ. Mesenchymal stem cells differentiate into tenocytes by bone morphogenetic protein (BMP) 12 gene transfer. *J Biosci Bioeng*. 2005;100(4):418-422.
25. Wikaninrum R, Highton J, Parker A, et al. Pathogenic mechanisms in the rheumatoid nodule: comparison of proinflammatory cytokine production and cell adhesion molecule expression in rheumatoid nodules and synovial membranes from the same patient. *Arthritis Rheum*. 1998;41(10):1783-1797.
26. Williams IF, Heaton A, McCullagh KG. Cell morphology and collagen types in equine tendon scar. *Res Vet Sci*. 1980;28(3):302-310.
27. Yao J, Woon CY, Behn A, et al. The effect of suture coated with mesenchymal stem cells and bioactive substrate on tendon repair strength in a rat model. *J Hand Surg Am*. 2012;37(8):1639-1645.